Pharm Res (2015) 32:779–792
DOI 10.1007/s11095-013-1231-0

RESEARCH PAPER

The Narrow-Spectrum HDAC Inhibitor Entinostat Enhances NKG2D Expression Without NK Cell Toxicity, Leading to Enhanced Recognition of Cancer Cells

Shiguo Zhu • Cecele J. Denman • Zehra S. Cobanoglu • Simin Kiany • Ching C. Lau • Stephen M. Gottschalk • Dennis P. M. Hughes • Eugenie S. Kleinerman • Dean A. Lee

Received: 24 April 2013 / Accepted: 14 October 2013 / Published online: 8 November 2013
© Springer Science+Business Media, LLC (outside the USA) 2013

ABSTRACT

Purpose Natural killer (NK) cell cytotoxicity correlates with the ligation of activating receptors (e.g., NKG2D) by their ligands (e.g., MHC class I–related chains [MIC] A and B) on target cells. Histone deacetylase inhibitors (HDACi) at high concentrations inhibit tumor growth and can increase NKG2D ligand expression on tumor targets, but are widely regarded as toxic to NK cells.

Methods We investigated the mechanism of entinostat, a benzamide-derivative narrow-spectrum HDACi, in augmenting the cytotoxicity of NK cells against human colon carcinoma and sarcoma by assessing gene and protein expression, histone acetylation, and cytotoxicity in *in vitro* and murine models.

Results We observed that entinostat dose- and time-dependent increase in MIC expression in tumor targets and NKG2D in primary human NK cells, both correlating with increased acetylated histone 3 (AcH3) binding to associated promoters. Entinostat pretreatment of colon carcinoma and sarcoma cells, NK cells, or both led to enhanced overall cytotoxicity *in vitro*, which was reversed by NKG2D blockade, and inhibited growth of tumor xenografts. Lastly, we showed decreased expression of MICA and ULBP2 transcription in primary human osteosarcoma.

Conclusions Entinostat enhances NK cell killing of cancer cells through upregulation of both NKG2D and its ligands, suggesting an attractive approach for augmenting NK cell immunotherapy of solid tumors such as colon carcinoma and sarcomas.

KEY WORDS cancer · HDAC inhibitor · natural killer cells · NKG2D · NKG2D ligands

ABBREVIATIONS

7-AAD	7-Amino-actinomycin D
AcH3	acetylated histone 3
AcH4	acetyl-histone 4
APC	allophycocyanin
ChIP	chromatin immunoprecipitation
FFLuc	firefly luciferase
HDAC	Histone deacetylase
HDACi	Histone deacetylase inhibitors
MIC	MHC class I–related chains
SAHA	suberoylanilide hydroxamic acid

Electronic supplementary material The online version of this article (doi:10.1007/s11095-013-1231-0) contains supplementary material, which is available to authorized users.

S. Zhu (✉)
Shanghai University of Traditional Chinese Medicine
School of Basic Medical Sciences, Shanghai, China
e-mail: jusco105@hotmail.com

C. J. Denman • Z. S. Cobanoglu • S. Kiany • D. P. M. Hughes • E. S. Kleinerman • D. A. Lee
Division of Pediatrics
The University of Texas MD Anderson Cancer Center
Houston, Texas, USA

C. C. Lau
Hematology/Oncology Section, Department of Pediatrics
Baylor College of Medicine, Houston, Texas, USA

S. M. Gottschalk
Baylor College of Medicine, Department of Pediatrics
Center for Cell and Gene Therapy
Texas Children's Cancer Center Houston, Texas, USA

D. A. Lee (✉)
Pediatrics Unit #853 University of Texas MD Anderson Cancer Center
1515 Holcombe Boulevard, Houston, Texas 77030-4009, USA
e-mail: dalee@mdanderson.org

ULBP UL16-binding proteins
VPA valproic acid

INTRODUCTION

Adoptive transfer of activated autologous or allogeneic NK cells has emerged as a safe and potentially efficacious immunotherapy for cancer (1). Although the clinical benefit of NK cells has been most pronounced for hematologic malignancies in the haploidentical hematopoietic stem cell transplant setting, there is growing evidence for NK cell activity against carcinomas and sarcomas (2). NK cells are a subset of peripheral-blood lymphocytes defined by the expression of CD56 and/or CD16 and the absence of the T-cell receptor CD3 . NK cells play a crucial role in the innate immune response to viruses and tumors, differentiating infected or malignant cells from normal "self" cells by a complex balance between receptor and ligand interactions (3). NK cell–mediated lysis correlates with the surface expression of activating and inhibitory receptors on NK cells and of the corresponding ligands on tumor cells. Accordingly, modulation of NK cell receptors and/or ligands is a recognized immune escape mechanism in oncogenesis (4). Thus, approaches that alter the balance of signals in favor of tumor cell killing, referred to as immunosensitization, are attractive as adjuncts to cell therapy.

NKG2D is the primary activating receptor of NK cells against tumor targets. It binds to a variety of target cell ligands, including MHC class I–related genes (MIC) A and B and UL16-binding proteins (ULBP) 1 through 5 (5), which are heterogeneously expressed on human cancers cells (4) and are upregulated in response to cellular stress. Surface expression of NKG2D depends on coexpression of the adapter protein DAP10 (6) and can be regulated by the cytokines IL-2, -7, -15, and -21 (7,8). Tumors may escape NK cell recognition by suppression of their NKG2D ligands or by indirect mechanisms that suppress NKG2D on NK cells (9). Recurrent and metastatic tumors such as sarcomas are marginally responsive to chemotherapy or radiation, but several studies have suggested that these tumors may be immunologically responsive (10). NK cells have activity against tumors (2,11), although the activity is widely variable and correlates with NK ligand expression (10). Therefore, an effective approach to cancer immunotherapy would be to restore the expression of NKG2D on NK cells or of its ligands on cancer cells.

In addition to direct cytotoxic or chemosensitizing effects, histone deacetylase (HDAC) inhibitors (HDACi) can modulate NK cell ligand expression. The HDACi trichostatin upregulates MICA and MICB in acute myeloid leukemia (12) and in acute lymphoid leukemia cells (13) by a direct mechanism of chromatin remodeling. In contrast, sodium valproate upregulates MICA and MICB expression in hepatoma cells by an indirect mechanism involving glycogen synthase-3 [GSK-3] (14), and increases NKG2D ligands in acute myelogenous leukemia cells (15). Upregulation of MICA and MICB by sodium butyrate may also be by an indirect mechanism, *via* increased transcription factors HSF1 and Sp1 (16). In each of these cases the increase in NKG2D ligands resulted in a corresponding increase in susceptibility to NK cell lysis. In addition, the HDACi depsipeptide, in combination with bortezomib, immunosensitized carcinomas to NK cell lysis by a mechanism associated with tumor necrosis factor–related apoptosis-inducing ligand (TRAIL) (17). These findings suggested that HDACi can be used as immune-enhancing antitumor agents that upregulate the expression of NKG2D ligands on tumor cells. Importantly, however, the HDACi valproic acid (VPA), romidepsin, suberoylanilide hydroxamic acid (SAHA), sodium butyrate, and trichostatin have all been shown to be toxic to NK cells *in vitro* at therapeutically relevant concentrations (18,19). Entinostat (MS-27-275, MS-275, SNDX-275) is a synthetic benzamide derivative that is specific for HDAC isoforms 1, 2, and 3 (Class I). Entinostat has shown activity against several human tumors (20) including pediatric osteosarcoma (21), and augments T cell responses to vaccination (22,23). Like other HDACi, entinostat can increase expression of NK cell ligands (24), but its direct effect on NK cells has not been described.

Here we demonstrate that entinostat enhances NK cell activity against colon carcinoma and sarcomas through both receptor and ligand modulation, and we determined the mechanism of receptor-ligand modulation by assessing transcriptional, translational, and epigenetic effects of entinostat on primary human NK cells,colon carcinoma and sarcoma cell lines both *in vitro* and *in vivo*.

MATERIALS AND METHODS

Cells

HCT-15 (colon carcinoma) and COL (neuroblastoma) were obtained and cultured as previously described (25). SaOS2 (osteosarcoma) was obtained from ATCC. CCH-OS-D and CCH-OS-T (osteosarcoma) were established by D.H. under an IRB-approved protocol at MD Anderson Cancer Center. CCH-OS-D was obtained from a core needle biopsy from an untreated teenage male presenting with a large proximal tumor primary and multifocal pulmonary and bone metastasis. CCH-OS-T was created from a malignant pleural effusion from a heavily pretreated patient with widespread metastatic osteosarcoma. HT1080 (fibrosarcoma) was retrovirally modified to express the eGFP-firefly luciferase fusion protein as previously described (26). Tumor cell lines were cultured in Dulbecco's modified Eagle's medium (DMEM) supplemented with 10% fetal bovine serum and 1% penicillin and streptomycin in 5% CO_2, and periodically

verified free of mycoplasma using MycoAlert (Lonza, Basel, Switzerland). Cell lines were validated by STR DNA fingerprinting using the AmpFℓSTR Identifiler kit according to manufacturer instructions (Applied Biosystems cat 4322288). The STR profiles were compared to known ATCC fingerprints (ATCC.org), to the Cell Line Integrated Molecular Authentication database (CLIMA) version 0.1.200808 (http://bioinformatics.istge.it/clima/) (Nucleic Acids Research 37:D925-D932 PMCID: PMC2686526) and to the MD Anderson fingerprint database. The STR profiles were last performed on October 15, 2010, and matched the reference DNA fingerprints or were unique (CCH-OS-D and CCH-OS-T).

Anonymized normal human donor buffy coats were obtained from the Gulf Coast Regional Blood Center (Houston, TX) under an IRB-approved protocol at MD Anderson Cancer Center. NK cells were enriched from buffy coats with RosetteSep Human NK Cell Enrichment Cocktail from StemCell Technologies, Inc. (Vancouver, BC, Canada), using 10 μL per 1 mL of buffy coat, which consistently yielded <5% $CD3^+$ content as assessed by flow cytometry. When necessary, a second purification step using RosetteSep by the method of Warren *et al.* was performed to further enrich the CD56+ content to ≥90% (27). Freshly isolated NK cells were cultured overnight, as indicated, in RPMI 1640 medium supplemented with 10% fetal bovine serum, 2 mM L-glutamine, and 1% penicillin and streptomycin. NK cells were expanded using the modified K562 cell line Clone9.mbIL21 as described (28).

Normal human mesenchymal stromal cells (MSC) were obtained from the Tulane Center for Gene Therapy. Human pulmonary artery endothelial cells (HPAEC) were obtained from Sciencell (Carlsbad, CA). Normal human fibroblasts were cultured directly from skin biopsy samples obtained under a research protocol approved by the Institutional Review Board of Baylor College of Medicine. These adherent cell lines were cultured for fewer than 5 passages, in conditions as described above.

Reagents

Entinostat was purchased from Sigma-Aldrich (St. Louis, MO) and dissolved in DMSO as a stock solution and further diluted in DMSO for working solutions. Of note, 0.1 μM entinostat approximates the low-end serum concentrations achieved in early-phase clinical trials (29). Higher concentrations were used to demonstrate dose responsiveness or assess toxicity. Romidepsin was obtained through the institutional pharmacy. PCI-24781 was obtained from Selleck-Pfizer (Houston, TX).

Antibodies

Murine anti-human MICA/B-PE, CD56-FITC, and CD107α-APC, goat anti-mouse-FITC, and murine isotype control IgG2a-PE, IgG1 κ-FITC, and IgG1 κ-APC, and 7-AAD were obtained from BD Biosciences. Murine anti-human ULBP1, ULBP2, ULBP3, and actin were purchased from Santa Cruz Biotechnology (Santa Cruz, CA). Murine anti-human acetyl-histone 3 (AcH3), acetyl-histone 4 (AcH4), HDAC1, HDAC2, and HDAC3 were obtained from Millipore (Temecula, CA). Murine anti-human NKG2D (unlabeled and PE-labeled) were obtained from R&D Systems (Minneapolis, MN).

Flow Cytometry

For surface direct staining, cells were exposed to appropriate antibodies for 30 min at 4°C, washed, and resuspended in staining buffer. For surface indirect staining, cells were first exposed to the primary antibodies (anti-NKG2D, anti-ULBP1, anti-ULBP2, or anti-ULBP3) for 30 min at 4°C, washed, and then stained with secondary goat anti-mouse IgG1-FITC for 30 min at 4°C. Data were acquired using a FACSCalibur cytometer (BD Biosciences)) and analyzed using FlowJo software (Ashland, OR).

Real-Time Polymerase Chain Reaction

Total RNA was isolated from human cultured primary NK cells using a SurePrep TrueTotal RNA Purification Kit (Fisher Scientific, Bridgewater, NJ) following the manufacturer's instructions. Samples were analyzed by quantitative RT-PCR with the iCycler (Bio-Rad, Hercules, CA) using a TaqMan One-Step RT-PCR Master Mix Reagents Kit (Applied Biosystems, Foster City, CA) and TaqMan gene expression primer sets for DAP10 (Hs99999901_s1) and 18S rRNA (Hs01548438_g1, Applied Biosystems).

Cell Proliferation and Viability

To investigate the effect of entinostat on the proliferation and viability of tumor cells, the MTT assay was performed. HCT-15 cells (2.5×10^3) or primary NK cells (1×10^5) were seeded per well in 96-well plates. The following day, entinostat was added at the indicated final concentration (0, 0.1, 1.0, and 10 μM). At 24, 48, and 72 h after addition of entinostat, MTT (Sigma-Aldrich, St. Louis, MO) was added to a final concentration of 0.5 mg/mL. After 4 h of incubation, the medium was aspirated, and an equal volume of DMSO was added to dissolve the formazan precipitate. Absorbance at 570 nm was determined using a SpectraMax Plus^{384} spectrophotometer (Molecular Devices, Sunnyvale, CA). Number and viability of cells exposed to HDAC inhibitors were determined using the Vi-CELL Analyzer (Beckman-Coulter) .

Cytotoxicity Assay

NK cell cytotoxicity was determined using the calcein release assay, a fluorometric assay comparable to the chromium release assay in determining NK cell cytotoxicity . Target cells or NK cells were incubated with entinostat or DMSO for 24 h. Target cells were labeled with 2 μg/mL calcein-AM (Sigma-Aldrich) for 1 h at 37°C with occasional shaking. Effector cells and target cells were co-cultured at the indicated effector-to-target (E:T) ratios (ranging from 40:1 to 5:1) and incubated at 37°C for 4 h. In blocking experiments, 10 μg/mL mouse anti-human NKG2D mAb or mouse IgG isotype control was added to NK cells 30 min before the co-culture. After incubation, 100 μL of the supernatant was harvested and transferred to a new plate. Absorbance at 570 nm was determined using a SpectraMax Plus^{384} spectrophotometer. The percent lysis was calculated according to the formula [(experimental release − spontaneous release)/(maximum release–spontaneous release)] × 100.

Degranulation Assay

Primary NK cells or HCT-15 cells were cultured in 0.1 μM entinostat for 24 h. Effector cells and target cells were co-cultured at a 1:1 ratio. CD107α-APC or isotype IgG-APC was added. Co-cultures were incubated for 4 h at 37°C. In blocking experiments, 10 μg/mL mouse antihuman NKG2D mAb or mouse IgG isotype control was added to NK cells 30 min before the co-culture. After 4 h of incubation, cells were stained with CD56-FITC, and NK cell degranulation was assessed by flow cytometry.

Western Blot Analysis

Cells were incubated as indicated with entinostat or DMSO for 24 h and then were lysed with 50 mM Tris-Cl (pH 6.8), 100 mM dithiothreitol, 2% SDS, and 10% glycerol. Samples were analyzed by SDS-PAGE, followed by immunoblotting using ChemiGlow chemiluminescent substrate (Alpha Innotech, San Leandro, CA) according to the manufacturer's instructions.

Histone Deacetylase Activity

HCT-15 Cells were incubated in 0.1 μM entinostat or DMSO for 24 h, and then co-immunoprecipitation was performed following the protocol of the Immunoprecipitation Kit (Protein G) (Roche Applied Science, Indianapolis, IN) after incubation with 4 μg of anti-human HDAC1 mAb, anti-human HDAC2 mAb, or mouse IgG. HDAC activity of the immunoprecipitated protein complexes was determined using the HDAC Assay Kit (Millipore). Briefly, the immunoprecipitated protein complexes were incubated with the HDAC Assay Substrate for 1 h at 37°C. The supernatant was then incubated with the HDAC Activator Solution for 30 min at room temperature. Fluorescence of each sample was determined using the SpectraMAX Gemini EM (Molecular Devices, Sunnyvale, CA) at 355 nm excitation and 460 nm emission. HDAC activity was calculated as the fluorescence ratio of HDAC-specific complex to isotype-precipited complex.

Chromatin Immunoprecipitation

HCT-15 cells or primary NK cells were incubated with 0.1 μM entinostat or DMSO for 24 h, and then chromatin immunoprecipitation (ChIP) was performed according to the protocol of the ChIP Assay Kit (Upstate Biotechnology, Lake Placid, NY). Briefly, HCT-15 cells or primary NK cells were fixed with 1% formaldehyde, pelleted, and resuspended in SDS lysis buffer. Chromatin was sonicated to 200- to 1,000-bp fragments using a Sonifier 250 (Branson Ultrasonics, Danbury, CT). Immunoprecipitation was performed at 4°C by overnight incubation with anti-AcH3, anti-AcH4, and rabbit IgG (control). Immune complexes were collected on protein A–agarose in a solution containing 0.4 μg/μL sonicated salmon sperm DNA and eluted. Cross-linking was reversed by heating overnight at 65°C. DNA was purified and subsequently analyzed by qPCR with the iCycler using SYBR Green RT-PCR Kit (Valencia, CA). A 233-bp fragment of the MICA proximal promoter spanning the region from –215 to +18, a 220-bp fragment of the MICB proximal promoter spanning bases –239 to –20, and a 233-bp fragment of the DAP10 proximal promoter spanning bases –332 to –99 were amplified using the following primers: MICA forward 5′-TTA GGC TGC GCT CCC GCG TGC TCC-3′, reverse 5′-CTC AGC GGC TCA AGC AGT GGC CGG-3′; MICB forward 5′-GTT TGG AGC TGT ACT CTC AGC TAC-3′, reverse 5′-CCC GCT CAG CGA CCG CTT ATC CAG-3′; DAP10 forward 5′-TCC CTC TCA AAC ACA CCC ACA TTC-3′, reverse 5′-CCT GCT GGT GTC AAG GCC ATC TGC-3′. The promoter regions, start codons, primer regions and amplicons are shown in Supplementary Material Figure S1. The amount of MICA, MICB, and DAP10 promoter-related sequence present in each reaction was calculated relative to a standard curve obtained using a serial 2-fold dilution of human genomic DNA. Results were expressed as the ratio of DNA immunoprecipitated by specific antibody and control IgG.

Tumor Mouse Xenograft Models

Murine lung metastases were established in 6- to 8-wk-old NOD.Cg-*Rag1*^{tm1Mom}*Prf1*^{tm1Sdz}/SzJ mice (The Jackson Laboratory, Bar Harbor, Maine, Stock number 004848) by injecting 5×10^5 HT1080.eGFP-FFLuc tumor cells *via* tail

vein. Mice were treated with 752 ng entinostat *via* intraperitoneal administration (in 0.1 mL PBS), or 8×10^6 IL-2-activated NK cells (in 0.2 mL PBS) by tail-vein injection. Mice received entinostat, NK cells, or both on days 4, 11, and 18. The control group received no treatment. Animal procedures including tumor cells injection, *in vivo* bioluminescent imaging, NK cell adoptive transfer, entinostat administration, and euthanasia were approved by the IACUC at the University of Texas MD Anderson Cancer Center.

Bioluminescent Imaging (BLI)

Tumor volume was assessed by imaging isofluorane-anesthetized mice using the IVIS system (Xenogen, Alameda, CA). Images were obtained 15 min after intraperitoneal injection of 1.5 mg (approx. 75 mg/kg) D-luciferin (Xenogen) in 0.1 mL of PBS. The light emitted by luciferase-expressing tumors was quantified using Living Image Version 2.50 (Wavemetrics, Inc., Lake Oswego, OR). A heatmap image corresponding to photons/second/cm^2/steradian (blue lowest and red highest) was superimposed over the reflected-light image of the animals for tumor localization. A rectangular region of interest (ROI) encompassing the mouse head and body was replicated between images, images were adjusted to identical luminescent scales, and bioluminescence reported as total flux for the region in photons/sec. Animals were imaged on day 12, 15, 18, 23, and 27.

Microarray Gene Expression Analysis

Osteosarcoma biopsy samples were obtained from under a research protocol approved by the IRB of Baylor College of Medicine. Total mRNA was extracted from frozen osteosarcoma patient samples, T7-amplified using oligo(dT) primers, and hybridized to microarray slides as previously described (30). The dataset from 83 patient samples was queried for NK cell ligands and expression was normalized to microarray expression data from normal osteoblasts.

Statistical Analysis

Results are expressed as the mean ± SD. Student's *t* test was performed for pair-wise comparisons, and Mann–Whitney *U* test with Bonferroni correction for intergroup comparisons. To examine group effects and account for variability of NK cell activity between donors, lysis of target cells was normalized to that of the untreated cells, adjusted for dose (E:T ratio), and analyzed in a multiple linear regression model. *In vivo* bioluminescent data was normalized for each animal to the first data point, in order to account for variability in tumor formation. Normalized tumor growth over time was compared between groups using Two-way Repeated Measures ANOVA and Bonferroni post-test correction for significance of intergroup comparisons. The Wilcoxon Signed Rank Test was used to determine if differences in gene expression were statistically different than the null hypothesis zero difference. Statistical analysis was performed using Prism 5 for Mac Os X, version 5.0c (GraphPad Software, La Jolla, CA). *P* values less than 0.05 (*), less than 0.01 (**), less than 0.001 (***), or less than 0.0001 (****) were considered significant.

RESULTS

Entinostat Causes a Time- and Concentration-Dependent Increase in MICA/B Expression on Human Cancer Cells

Based on previous reports that HDACi could sensitize tumor cells to NK cell lysis, we screened a panel of HDACi (VPA, entinostat, SAHA, TSA, romidepsin, and PCI24781) for their ability to enhance NK cell lysis of tumor targets (not shown). Entinostat effectively increased target cell lysis at concentrations as low as 0.1 μM, which corresponds to pharmacologically relevant doses (20,21,29), and we therefore sought to characterize the mechanism of this immunosensitization. Because NK cell activation is determined by the balance of activating and inhibitory ligands on the target cell, we measured the effect of entinostat on the expression of NKG2D ligands (NKG2D-L) on HCT-15 cells. As demonstrated by flow cytometry, the surface expression of MICA/B increased after 24 h of exposure to entinostat in a concentration-dependent manner (Fig. 1a) compared to DMSO vehicle control. MICA/B expression steadily increased over a 72-h period when HCT-15 cells were continuously exposed to 0.1 μM entinostat as compared to DMSO (Fig. 1b). We then assessed NKG2D-L expression on six sarcoma cell lines treated for 24 h with DMSO or 0.1 μM entinostat and found that while baseline expression was variable, MICA/B and ULBP2 were positively affected by treatment (Fig. 1e).

Entinostat Causes a Time- and Concentration-Dependent Increase in NKG2D Expression on Primary Human NK cells

Since the expression of ligands for NK cell activation was increased by entinostat, we tested whether the corresponding receptor on NK cells, NKG2D, was also affected by entinostat. While NKG2D is expressed at a low level in resting human NK cells, activation with cytokines can increase expression rendering NK cells more cytotoxic to MICA/B- or ULBP-expressing targets. We found that entinostat increased the surface expression of NKG2D on purified

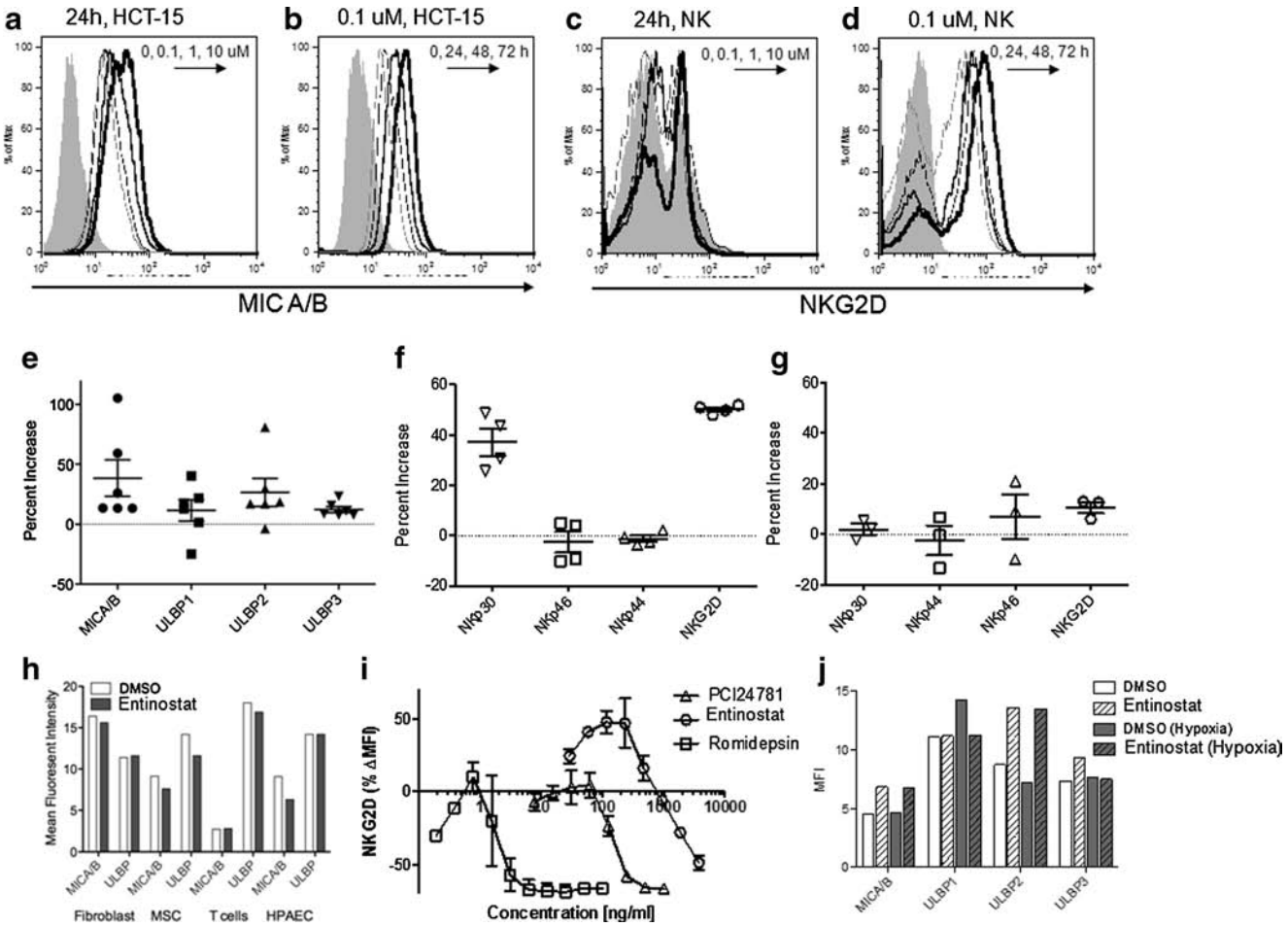

Fig. 1 *Dose response and kinetics of entinostat induction of NKG2D in fresh primary NK cells and of NKG2D ligands in tumor cell lines*. (**a**) Dose response of MICA/B expression in HCT-15 cells 24 h after incubation with entinostat (0, 0.1, 1, and 10 μM). (**b**) Kinetics of MICA/B expression in HCT-15 cells 24, 48, and 72 h after incubation with 0.1 μM entinostat. (**c**) Dose response of NKG2D expression in primary human NK cells 24 h after incubation with entinostat (0, 0.1, 1, and 10 μM). (**d**) Kinetics of NKG2D expression on NK cells 24, 48, and 72 h after incubation with 0.1 μM entinostat. Flow histograms: Gray shaded, isotype control antibody. *Thin gray line*, control cells treated with DMSO (*a*, *c*) or assessed at time 0 h (*b*, *d*). *Black thin*, *medium*, or *thick lines* represent 0.1, 1, and 10 μM respectively (*a*, *c*) or 24, 48, and 72 h respectively (*b*, *d*). (**c**) and (**d**) are representative of experiments with five different NK cell donors. (**e**) Increase in NKG2D ligands in HCT-15, SaOS2, COL, LM7, CCH-OS-D, and CCH-OS-T 24 h after incubation with 0.1 μM entinostat. (**f**) Increase in NKG2D, NKp30, NKp44, and NKp46 after 24 h incubation with 0.1 μM entinostat in freshly-isolated NK cells, or (**g**) in NK cells expanded with IL-2 and IL-21. (**h**) Expression of MICA/B and ULBP (pooled) on normal human cells in culture for 24 h with or without 0.1 μM entinostat. (**i**) Change in expression of NKG2D after 24 h incubation with different concentrations of entinostat (31.2, 62.5, 125, 250, 500, 1000, 2000 and 4000 ng/mL), romidepsin (0.195, 0.39, 0.78, 1.56, 3.12, 6.25, 12.5, 25, 50 and 100 ng/mL), or PCI-24781(7.8, 15.6, 31.2, 62.5, 125, 250, 500 and 1000 ng/mL). (**j**) Expression of NKG2D ligands in tumor cells as determined by MFI after 24 h culture at 21% or 1% O_2, with or without 0.1 μM entinostat. Mean ± SEM are shown (**e**, **f**, **g**, **i**).

human NK cells in a concentration-dependent manner (Fig. 1c). When NK cells were exposed to 0.1 μM entinostat for 72 h, NKG2D expression as measured by mean fluorescence intensity increased up to 5 times that of control DMSO-treated cells (Fig. 1d). When we assessed independent donors for NK cell receptor expression following 24 h treatment with 0.1 μM entinostat, we found a significant increase in the activating receptor NKp30 and NKG2D expression (Fig. 1f), as well as a modest increase in KIR expression (not shown). There was no increase in the activating receptors NKp44 or NKp46. In NK cells that had been expanded in the presence of IL-2 and IL-21 stimulation, having high baseline receptor expression, entinostat was able to further augment NKG2D expression (Fig. 1g).

Entinostat Does Not Increase NKG2D-L Expression in Normal Cells

A generalized increase in NKG2D-L expression on normal cells could lead to unwanted NK cell reactivity. We therefore assessed the ability of entinostat to increase NKG2D-L on normal human fibroblasts, mesenchymal stem cells, T cells, and peri-aortic epithelial cells. We found very low expression of NKG2D-L on normal cells, and in no case did we observe

an increase in expression after treatment with entinostat (Fig. 1h).

Unlike Other Narrow-Spectrum HDACi, Entinostat Induces NKG2D Activation Over a Broad Concentration Range

Since entinostat is a narrow-spectrum HDAC inhibitor effecting mostly HDAC1 and HDAC3, we compared the induction of NKG2D expression by entinostat with that of PCI-24781 (HDAC1/HDAC3>HDAC 2>HDAC1) and romidepsin (HDAC1/HDAC2) across their range of pharmacologically-relevant concentrations. PCI-24781 and romidepsin in the indicated concentrations were not able to induce NKG2D expression, whereas entinostat was effective across a 30-fold concentration range (Fig. 1i).

Entinostat is Effective in Inducing NKG2D Ligands in Hypoxic Conditions

Recognizing that solid tumors are characterized by relative hypoxia, we tested whether NKG2D ligands were differentially expressed and whether entinostat was effective in upregulation under hypoxic conditions. HCT-15 cells were grown under standard tissue culture conditions in 21% O_2 or under hypoxic conditions using constant-flow premixed 1% O_2 in N_2. We found similar levels of baseline NKG2D ligand expression, and entinostat was equally effective in raising expression levels of MICA/B and ULBP2 (Fig. 1j).

Low-Concentration Entinostat Increases HDAC Activity, Resulting in Enhanced Acetylation of Histones H3 and H4 in Tumor Cells and NK Cells

Small-molecule inhibitors of enzyme activity often have effects that occur through secondary mechanisms. To determine whether entinostat increased cell-surface NKG2D and MICA/B through a direct epigenetic effect on expression of these genes, we first assessed whether the 0.1-μM concentration was able to affect HDAC activity and then determined levels of HDAC expression and histone acetylation by Western blotting. We found that entinostat at this low concentration inhibited activity of HDAC1 and HDAC2 (Fig. 2a) without affecting their expression (Fig. 2b) and that this inhibition led to a marked increase in acetylation of histones 3 (AcH3) and 4 (AcH4) in both NK cells and HCT-15 (Fig. 2b).

Entinostat Increases Binding of AcH3 and AcH4 to MICA, MICB, and DAP10 Promoters, Leading to Increased DAP10 Transcription in Primary NK Cells

Since clear modification of histone acetylation was observed in both NK cells and HCT-15, we investigated whether this led directly to increased transcription of the NK receptors and ligands using chromatin immunoprecipitation (ChIP). Antibodies against AcH3 and AcH4 were used to precipitate associated chromatin before and after treatment with entinostat. For HCT-15, qPCR specific for the promoters of MICA and MICB (Supplementary Material Fig. S1) was performed to determine the relative association of these promoters with the acetylated histones, normalized to promoter content of total genomic DNA. Since the promoter for NKG2D has not been described, qPCR specific for the promoter of the NKG2D adapter molecule DAP10 (Supplementary Material Fig. S1) was used as a surrogate. We found enhancement of AcH3 binding to the promoters of MICA (Fig. 3a) and MICB (Fig. 3b) in HCT-15 cells treated with entinostat. We also found significant ($P<0.001$) enhancement of AcH3 and AcH4 binding to the promoters of DAP10 (Fig. 3c) in NK cells treated with entinostat. The transcriptional effect of enhanced AcH binding to the DAP10 promoter was confirmed using qPCR (Fig. 3d).

Entinostat Directly Inhibits Tumor Cell Growth and is Toxic NK Cells Only with Prolonged Exposure at High Concentrations

While increased NKG2D and NKG2D-L expression could predict enhanced tumor recognition, the effect on NK cell viability would negate this benefit and a large direct effect on tumor survival or proliferation could make an enhanced benefit difficult to observe. Therefore we assessed the affect of entinostat on the proliferation of HCT-15 as assessed by the MTT assay (Fig. 4a), and found that increased doses and exposures lead to decreased proliferation consistent with other reports (21). At lower concentrations or for shorter durations entinostat had a small but nonsignificant effect on cell growth compared with the effect of DMSO vehicle alone. Since the MTT assay can be affected by alterations in cell metabolism, we also assessed the proliferation of four osteosarcoma cell lines in response to entinostat using Vi-CELL viable cell counts after 72 h (Fig. 4b), and confirmed a strong anti-proliferative effect at higher concentrations but a marginal effect at 0.1 μM. Since NK cells have minimal proliferation in culture, we assessed the toxicity of entinostat on NK cells by flow cytometry for 7-AAD uptake. Although NK cells were more sensitive to higher concentrations and prolonged exposure of entinostat than osteosarcoma cells, 0.1 μM caused minimal loss in viability at 72 h (Fig. 4c).

Entinostat Enhances NK Cell Killing of Tumor Targets by an NKG2D-Dependent Mechanism

With evidence for increased expression of activating NK cell ligands and receptors, we determined whether this increased expression resulted in increased cytotoxicity, and whether the

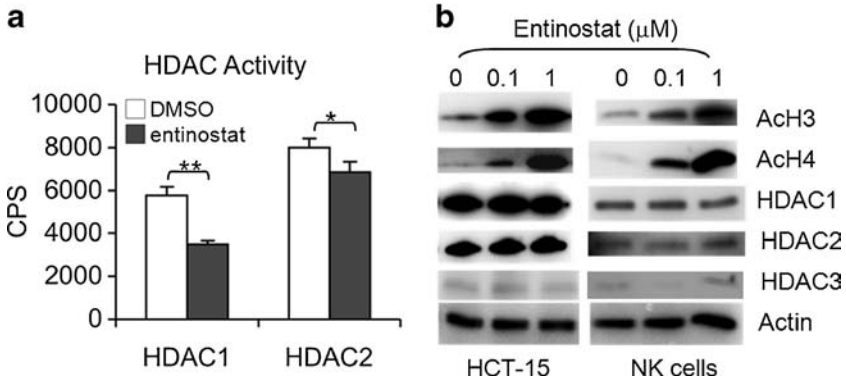

Fig. 2 *Effect of entinostat on deacetylation of histones H3 and H4, HDAC expression, and HDAC activity*. (**a**) HCT-15 cells were treated with 0.1 μM entinostat for 24 h, and the activity of HDAC1- or HDAC2-immunoprecipitated complexes were measured. HDAC activity shown is relative to the activity of control IgG immunoprecipitate. CPS, fluorescent counts per second. (**b**) HCT-15 or fresh primary NK cells were treated with entinostat for 24 h, and AcH3, AcH4, and HDAC1, 2, and 3 were detected by Western blotting. *, $P < 0.05$, **; $P \leq 0.01$; ***, $P \leq 0.001$.

effects on cytotoxicity were additive. We treated HCT-15, purified human NK cells, or both for 24 h with entinostat at the noncytotoxic concentration of 0.1 μM prior to co-culture and detection of cell killing by the calcein release assay. For all donors tested and at all effector:target (E:T) ratios, NK cell killing was enhanced by entinostat pretreatment of the HCT-15 cells, the NK cells, or both as compared to untreated cells (Fig. 5a). Since target cell lysis was already high at the higher E:T ratios, the synergy in cytotoxicity was more evident at lower E:T ratios. After adjusting for the contribution of dose (E:T ratio) under a multiple linear regression model, there remained a significant difference between treatment groups ($p = 0.019$). Dual-treatment (both NK cells and targets treated with entinostat) resulted in a greater increase in percent specific lysis than either entinostat treated NK cells ($p = 0.003$) or entinostat treated targets ($p < 0.001$). To demonstrate that target cell lysis by NK cells was dependent on activation *via* NKG2D, we used anti-NKG2D antibodies to block recognition of the cognate ligand, and showed that anti-NKG2D blockade fully reversed the entinostat–enhanced lysis of the target cells (Fig. 5b) to levels below that of untreated cells.

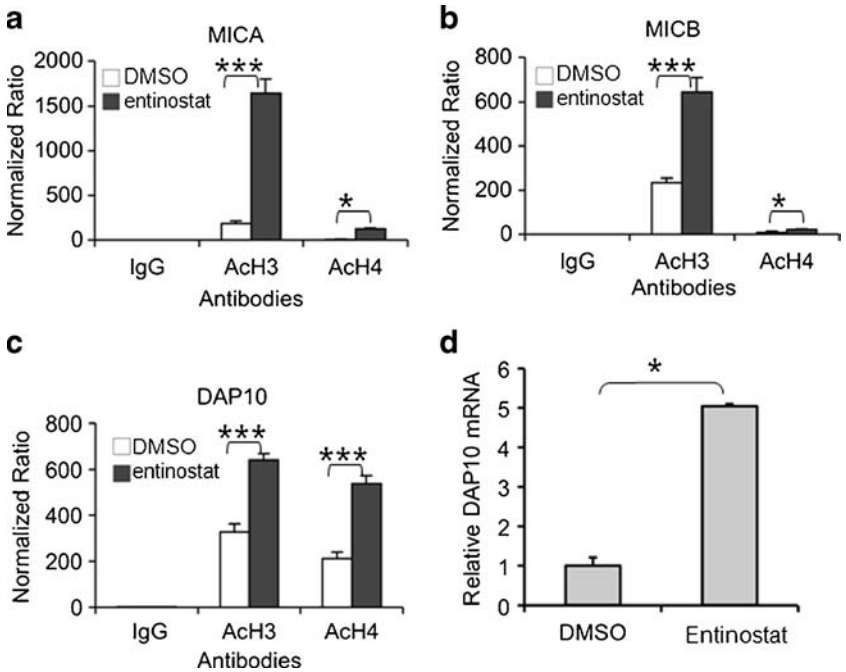

Fig. 3 *Effect of entinostat on MICA, MICB, and DAP10 transcription and promoter binding by acetylated histones*. Fresh primary human NK cells were treated with DMSO or 0.1 μM entinostat. Chromatin was immunoprecipitated with antibodies to acetylated histone 3 (AcH3) or 4 (AcH4) or isotype control IgG. Coimmunoprecipitation of the MICA (**a**), MICB (**b**), or the DAP10 promoter (**c**) was determined by qPCR, normalized to the promoter content of input genomic DNA, and shown as the ratio of promoter precipitated with specific antibody to promoter precipitated with control antibody. (**d**) Fresh primary human NK cells were treated with DMSO or 0.1 μM entinostat. DAP10 transcripts were determined by qRT-PCR relative to 18S RNA, and normalized to DMSO control. *, $P < 0.05$, **; $P \leq 0.01$; ***, $P \leq 0.001$.

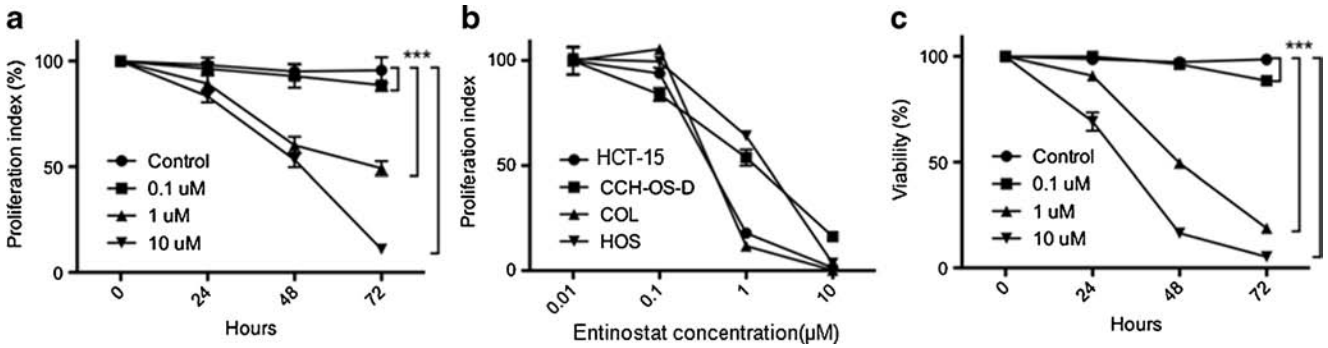

Fig. 4 *Direct effect of entinostat on proliferation of cancer cells or viability of NK cells*. (**a**) HCT-15 cells were cultured in indicated concentrations of entinostat for up to 72 h, and proliferation determined by MTT assay as indicated. (**b**) HCT-15, CCH-OS-D, COL and HOS cells were cultured in indicated concentrations of entinostat for 72 h, and viable cell number was determined using the Vi-cell assay and proliferation index calculated. (**c**) Freshly-isolated human NK cells were cultured in indicated concentrations of entinostat for up to 72 h, and viability was assessed by flow cytometry for 7-AAD uptake. *, $P < 0.05$, **; $P \leq 0.01$; ***, $P \leq 0.001$.

Low-Concentration Entinostat Enhances the Degranulation of NK Cells that Recognize Tumor Targets by NKG2D-Dependent Mechanisms

NK cell killing of target cells is mediated by the release of granules, containing granzymes and perforin, that are lined with lysosomal-associated membrane protein–1 (LAMP-1, CD107a). To confirm that the entinostat–enhanced killing of HCT-15 cells by NK cells was caused by NKG2D-mediated liberation of lytic effectors from the NK cells, we used flow cytometry to detect neoexpression of CD107a as a surrogate for NK cell degranulation. We first pretreated HCT-15 and/or purified human NK cells for 24 h with entinostat at the noncytotoxic concentration of 0.1 μM and then co-cultured the cells for 4 h in the presence of anti-CD107a before analysis. After first gating on the NK cell population by side- and forward-scatter, relative expression of CD107a was determined for both low- and high-CD56–expressing NK cell populations. Degranulation was enhanced for both NK cell populations after entinostat pretreatment of the HCT-15 cells (Fig. 5e), the NK cells (Fig. 5g), and both (Fig. 5f), and this degranulation was blocked to levels below that of untreated cells (Fig. 5d) by the addition of anti-NKG2D antibodies (Fig. 5j). Of note, although a majority of degranulating NK cells were of the $CD56^{low}$ phenotype (Fig. 5f), the $CD56^{hi}$ NK cells had a greater target-specific response to HCT-15 (Fig. 5a *vs.* Fig. 5f).

Tumor Xenografts Respond to Combined Treatment with Low-Dose Entinostat and NK Cells

Having established that entinostat sensitizes tumor targets to NK cell lysis *in vitro* by upregulation of NKG2D and its ligands, we determined if entinostat could augment adoptive immunotherapy for established tumors *in vivo* using a xenograft pulmonary metastatic model. To allow for serial imaging, we used the HT1080 fibrosarcoma lung metastasis model transduced with eGFP-firefly luciferase for bioluminescent imaging. Mice received no therapy or were treated on days 4, 11, and 18 with entinostat, NK cells, or entinostat and NK cells. Tumor growth was monitored by BLI on days 12, 15, 19, 23, and 27 (Fig. 6a, b). Since entinostat induces expression of the GFP-luciferase transgene (Supplementary Material Fig. S2), BLI measurements were normalized to pretreatment flux for each mouse (Fig. 6c). Mice treated with both entinostat and NK cells had a significantly lower tumor burden on day 27 as judged by BLI in comparison to controls, where as mice treated with entinostat or NK cells alone did not. These results confirm our *in vitro* studies, that entinostat sensitizes cancer cells to NK cell mediated killing.

NK Cell Ligand Expression is Downregulated in Human Osteosarcoma Samples

Having demonstrated the effect and mechanism of combined treatment of colon carcinoma and sarcoma with NK cells and HDACi, we questioned whether NKG2D-L downregulation was clinically relevant for cancer patients. We queried the database containing 83 microarrray gene expression profiles from osteosarcoma patients for known NKG2D cell ligands, and included NK cell KIR ligands, HLA, for comparison. We found that compared to normal osteoblasts human osteosarcoma samples have significantly and markedly downregulated expression of MICA/B and ULBP2 (Fig. 7). Although ULBP3 is also downregulated, it was so to a lesser degree. Although HLA-A and HLA-B were upregulated, the primary KIR ligand HLA-C was not significantly altered in expression.

DISCUSSION

In this study, we show that the HDACi entinostat not only increases the expression of the activating ligands MICA and

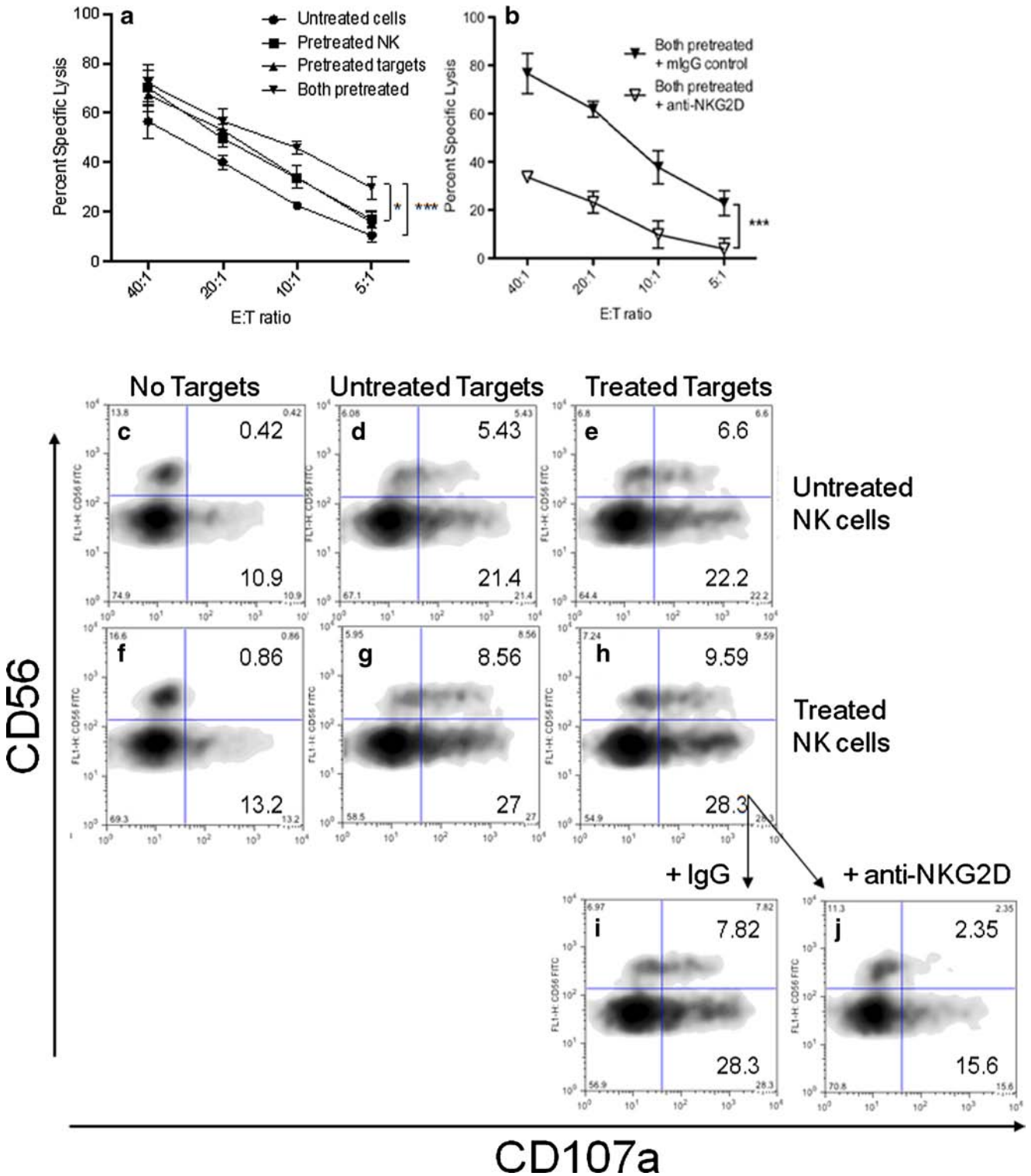

Fig. 5 *Effect of entinostat and NKG2D blockade on NK cell degranulation and killing of HCT-15 targets*. (**a**) HCT-15 and primary NK cells were treated overnight with DMSO or 0.1 μM entinostat, and then co-cultured in each combination as shown. Cytotoxicity was determined after 4 h co-culture using the calcein release assay. (**b**) As in (*a*), but NK cells were blocked with 10 mg/mL mouse IgG (closed circles) or mouse anti-human NKG2D prior to co-culture. Data shown are mean ± SEM for three independent donors. To assess NK cell degranulation, HCT-15 cells and primary NK cells were pretreated overnight and cocultured as above, followed by addition of anti-CD107a-PE and CD56-FITC, and then CD107a expression on NK cell surface was determined by FACS. (**c**) NK alone, (**d**) NK + HCT-15, (**e**) NK + treated HCT-15, (**f**) treated NK alone, (**g**) treated NK + HCT-15, (**h**), (**i**), (**j**) treated NK + treated HCT-15, where NK cells were blocked with 10 μg/mL of mouse IgG (*i*) or mouse antihuman NKG2D antibody (*j*) prior to co-culture. *, $P < 0.05$, **; $P \leq 0.01$; ***, $P \leq 0.001$.

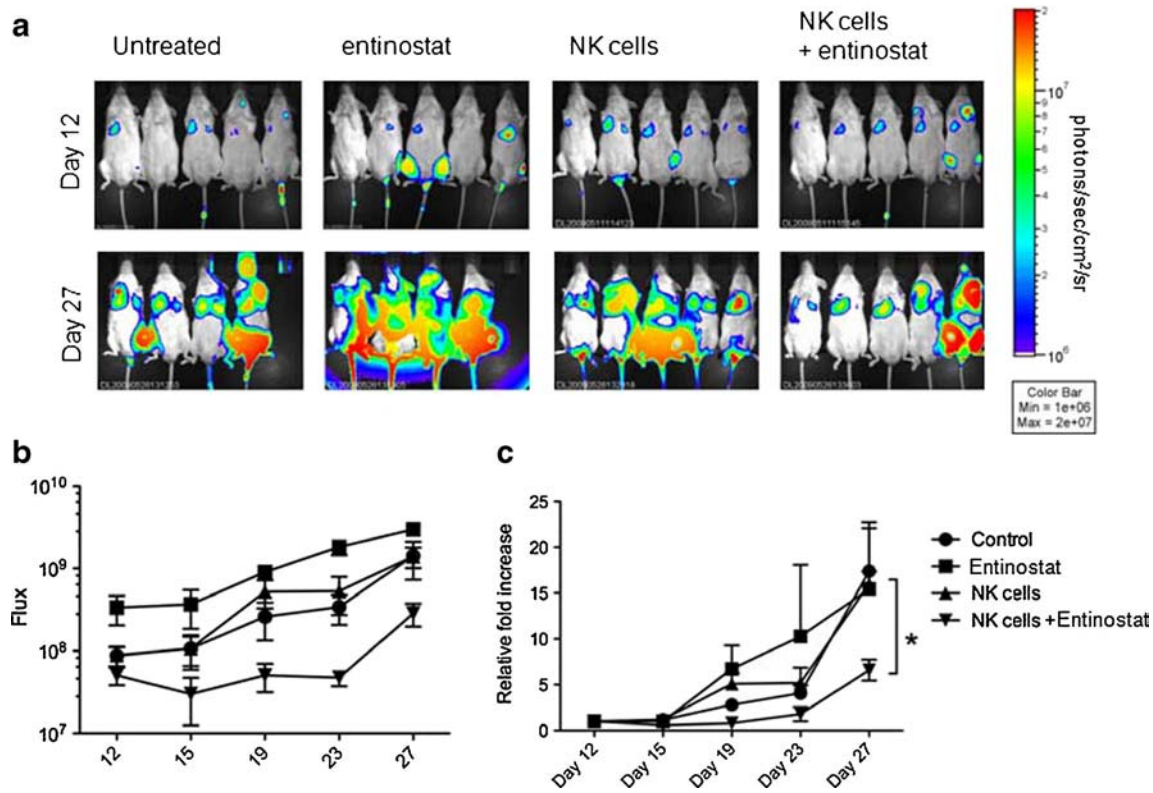

Fig. 6 *Synergism of entinostat and adoptively transferred NK cells on HT1080 fibrosarcoma pulmonary metastasis*. Mice were injected *via* tail vein with 10^5 HT1080-GFP-Luc cells on day 0. Mice were treated with 752 ng entinostat, 8×10^6 IL-2-activated NK cells, or both on 4, 11, and 18. Tumor size was assessed by BLI every 3 to 4 days beginning on day 12 (**a**, **b**). Flux for each mouse was normalized to day 12 (**c**). Figure is representative of two independent experiments. *, $P < 0.05$.

MICB on human cancer cells, but is novel in its ability to simultaneously increase the expression of the activating receptor NKG2D on primary human NK cells. We show that the upregulation of these activating receptors and ligands is a direct result of increased histone acetylation and binding of acetylated histones to relevant promoters, that their upregulation leads to enhanced NK cell cytotoxicity, and this enhanced NK cell cytotoxicity translates to improved treatment effect in a xenograft model.

NK cell survival and function are adversely affected by many chemotherapeutic agents . Indeed, Ogbomo *et al.* (18) demonstrated that HDACi can suppress NK cell lytic activity, potentially confounding their efficacy in cancer therapy. Entinostat was not included in their study, and in contrast, Kato *et al.* (31) demonstrated a synergistic effect between entinostat and IL-2 in a murine model of renal cell carcinoma and showed correlation of tumor inhibition with a reduction in splenic regulatory T cells in the treated mice. Although the investigators found no difference in NK cell numbers, NK cell function was not specifically tested.

The differences in reported effects of HDACi may be explained by their relative specificity for HDAC isoforms, and thus HDACi may also vary greatly in their ability to immunosensitize NK cells. Ogbomo *et al.* (18) used VPA (a broad-spectrum class I- and IIa-specific HDACi), and SAHA (a pan-HDACi), and found that expression of the natural cytotoxicity receptors NKp30, NKp44 and NKp46 was decreased but NKG2D expression was not significantly changed, resulting in impaired granule exocytosis. Importantly, this effect was noted at clinically relevant concentrations (0.25–1 mM and 0.5–2 μM for VPA and SAHA, respectively). In addition, entinostat, SAHA, and sodium butyrate were recently shown to increase NK cell killing of prostate carcinoma (PC3) and medulloblastoma (DAOY) cells. This was demonstrated at relatively high concentrations (2 and 10 μM for entinostat, 1 and 5 μM for SAHA), the mechanism was not established for entinostat, and the effect of the HDACi on NK cells was not determined (32). For SAHA, they demonstrated that the mechanism involved both NKp30 and NKG2D.

While it is difficult to extrapolate between *in vitro* concentrations and *in vivo* doses, here we have evaluated entinostat, a selective class I-specific HDACi (with primary activity against HDAC1 (33)), at concentrations below the $AUC_{0\text{-}24h}$ that was achieved in early-phase clinical trials without dose-limiting toxicity (20,21,34). To avoid variability in parenteral absorption, we used an IP dose of 752 ng (2 nmoles), for a calculated maximum peak concentration of

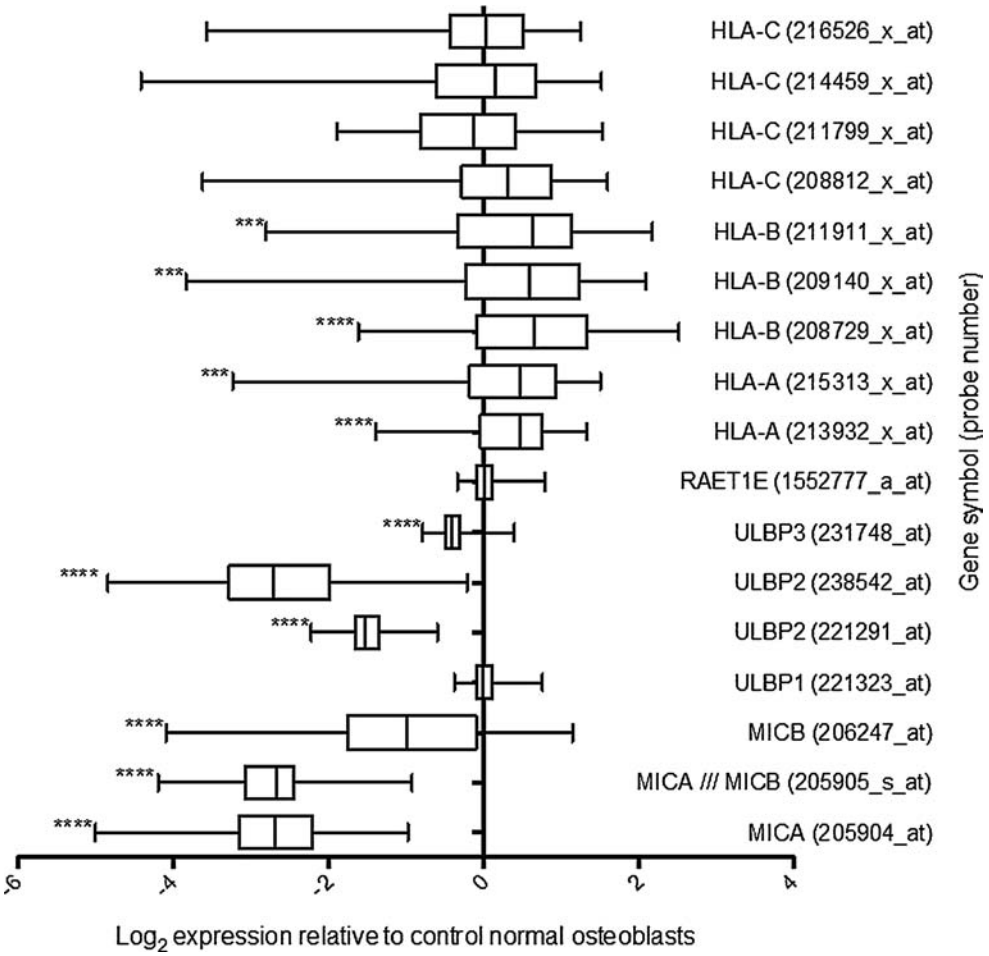

Fig. 7 *Expression of mRNA for NK cell ligands in patient osteosarcoma samples compared to normal osteoblasts*. Microarray gene expression data of 83 samples of human osteosarcoma were queried for known NK cell ligands. Each sample was normalized to the expression of normal human osteoblasts, and plotted as Log_2 expression (*box* = mean +/− SD, *whiskers* = range). Genes significantly under- or over-expressed are indicated: ***, $P \leq 0.001$, ****, $P \leq 0.0001$.

0.1 μM in a 25 g mouse (assuming total body water distribution). In the clinical trials, peak concentrations at 1 h after the highest tolerated doses (6 mg/m^2) varied widely with a median of 73 ng/mL (~2 μM), with sustained concentrations averaging 3 ng/mL (~0.1 μM) over the next 24 h (29), suggesting that our findings at 0.1 μM are clinically achievable with low toxicity. This level is also well within the serum concentrations achieved at tolerable doses in pediatric phase I trials (35). We found that a concentration of 0.1 μM entinostat was below the cytotoxic level for this drug but was sufficient to induce immunosensitization.

In addition to the direct immune evasion mechanism of downregulating activating ligands, cancers also demonstrate indirect mechanisms affecting NK cell function. For example, advanced-stage myelodysplastic syndrome is associated with impaired distal cytokine release (36), and NK cells from patients with breast carcinoma exhibit altered killer immunoglobulin-like receptor (KIR) expression (37). While the majority of recent NK cell adoptive transfer clinical trials have utilized HLA-haploidentical allogeneic donors, reversing NK cell dysfunction may enable endogenous NK cell function or autologous adoptive cell therapies after *ex vivo* expansion, as autologous NK cells can reject tumors independent of missing self if sufficient activating ligands are present (38).

Finally, we showed in human clinical osteosarcoma samples that MICA/B and ULBP2 are downregulated, and note that these same NKG2D-L are upregulated by entinostat, suggesting that this may be a common and treatable mechanism of immune escape for these tumors. In addition to augmenting the activation pathways for NK cell recognition of cancer cells, entinostat may also augment the cell death induction by NK cells through upregulation of FAS on cancer cells (39,40).

Taken together, our results indicate that selected HDACi, even at low doses that are not directly inhibitory to tumor cell growth, may alter both the effectors and targets of innate anticancer immune responses. Thus entinostat has the potential to enhance concurrent NK-cell therapy for solid tumors such as colon carcinoma and osteosarcoma.

ACKNOWLEDGMENTS AND DISCLOSURES

The authors acknowledge Laurence J. N. Cooper for initiating the discussions that led to this work, Joya Chandra

for sharing her expertise in epigenetics and critiquing the manuscript, and Shana Palla for guiding our statistical analysis. Financial support for this research was provided to D.A.L. and D.P.M.H. by the Brenda and Howard Johnson Fund, the Physician Scientist Program of MD Anderson Cancer Center, and the Sunbeam Foundation. Financial support to S.Z. was provided by the National Natural Science Foundation of China (81071858; 81273216) and Innovation Program of Shanghai Municipal Education Commission (11ZZ105). STR DNA fingerprinting was done by the Characterized Cell Line Core at MD Anderson Cancer Center, funded by NCI # CA16672. The MSC employed in this work were provided by the Tulane Center for Gene Therapy through a grant from NCRR of the NIH, Grant # P40RR017447.

REFERENCES

1. Miller JS, Soignier Y, Panoskaltsis-Mortari A, McNearney SA, Yun GH, Fautsch SK, *et al*. Successful adoptive transfer and in vivo expansion of human haploidentical NK cells in patients with cancer. Blood. 2005;105:3051–7.
2. Cho D, Shook DR, Shimasaki N, Chang YH, Fujisaki H, Campana D. Cytotoxicity of activated natural killer cells against pediatric solid tumors. Clin Cancer Res. 2010;16:3901–9.
3. Lanier LL. NK cell recognition. Annu Rev Immunol. 2005;23:225–74.
4. Pende D, Rivera P, Marcenaro S, Chang CC, Biassoni R, Conte R, *et al*. Major histocompatibility complex class I-related chain A and UL16-binding protein expression on tumor cell lines of different histotypes: analysis of tumor susceptibility to NKG2D-dependent natural killer cell cytotoxicity. Cancer Res. 2002;62:6178–86.
5. Sutherland CL, Rabinovich B, Chalupny NJ, Brawand P, Miller R, Cosman D. ULBPs, human ligands of the NKG2D receptor, stimulate tumor immunity with enhancement by IL-15. Blood. 2006;108:1313–9.
6. Wu J, Song Y, Bakker AB, Bauer S, Spies T, Lanier LL, *et al*. An activating immunoreceptor complex formed by NKG2D and DAP10. Science. 1999;285:730–2.
7. Roberts AI, Lee L, Schwarz E, Groh V, Spies T, Ebert EC, *et al*. NKG2D receptors induced by IL-15 costimulate CD28-negative effector CTL in the tissue microenvironment. J Immunol. 2001;167:5527–30.
8. Burgess SJ, Marusina AI, Pathmanathan I, Borrego F, Coligan JE. IL-21 down-regulates NKG2D/DAP10 expression on human NK and CD8+ T cells. J Immunol. 2006;176:1490–7.
9. Bubenik J. MHC class I down-regulation: tumour escape from immune surveillance? (review). Int J Oncol. 2004;25:487–91.
10. Mariani E, Tarozzi A, Meneghetti A, Cattini L, Facchini A. Human osteosarcoma cell susceptibility to natural killer cell lysis depends on CD54 and increases after TNF alpha incubation. FEBS letters. 1997;406:83–8.
11. Buddingh EP, Schilham MW, Ruslan SE, Berghuis D, Szuhai K, Suurmond J, *et al*. Chemotherapy-resistant osteosarcoma is highly susceptible to IL-15-activated allogeneic and autologous NK cells. Cancer Immunol Immunother. 2011;60:575–86.
12. Rohner A, Langenkamp U, Siegler U, Kalberer CP, Wodnar-Filipowicz A. Differentiation-promoting drugs up-regulate NKG2D ligand expression and enhance the susceptibility of acute myeloid leukemia cells to natural killer cell-mediated lysis. Leuk Res. 2007;31:1393–402.
13. Kato N, Tanaka J, Sugita J, Toubai T, Miura Y, Ibata M, *et al*. Regulation of the expression of MHC class I-related chain A, B (MICA, MICB) via chromatin remodeling and its impact on the susceptibility of leukemic cells to the cytotoxicity of NKG2D-expressing cells. Leukemia. 2007;21:2103–8.
14. Armeanu S, Bitzer M, Lauer UM, Venturelli S, Pathil A, Krusch M, *et al*. Natural killer cell-mediated lysis of hepatoma cells via specific induction of NKG2D ligands by the histone deacetylase inhibitor sodium valproate. Cancer Res. 2005;65:6321–9.
15. Diermayr S, Himmelreich H, Durovic B, Mathys-Schneeberger A, Siegler U, Langenkamp U, *et al*. NKG2D ligand expression in AML increases in response to HDAC inhibitor valproic acid and contributes to allorecognition by NK-cell lines with single KIR-HLA class I specificities. Blood. 2008;111:1428–36.
16. Zhang C, Wang Y, Zhou Z, Zhang J, Tian Z. Sodium butyrate upregulates expression of NKG2D ligand MICA/B in HeLa and HepG2 cell lines and increases their susceptibility to NK lysis. Cancer Immunol Immunother. 2009;58:1275–85.
17. Lundqvist A, Abrams SI, Schrump DS, Alvarez G, Suffredini D, Berg M, *et al*. Bortezomib and depsipeptide sensitize tumors to tumor necrosis factor-related apoptosis-inducing ligand: a novel method to potentiate natural killer cell tumor cytotoxicity. Cancer Res. 2006;66:7317–25.
18. Ogbomo H, Michaelis M, Kreuter J, Doerr HW, Cinatl Jr J. Histone deacetylase inhibitors suppress natural killer cell cytolytic activity. FEBS Lett. 2007;581:1317–22.
19. Kelly-Sell MJ, Kim YH, Straus S, Benoit B, Harrison C, Sutherland K, *et al*. The histone deacetylase inhibitor, romidepsin, suppresses cellular immune functions of cutaneous T-cell lymphoma patients. Am J Hematol. 2012;87:354–60.
20. Saito A, Yamashita T, Mariko Y, Nosaka Y, Tsuchiya K, Ando T, *et al*. A synthetic inhibitor of histone deacetylase, MS-27-275, with marked in vivo antitumor activity against human tumors. Proc Natl Acad Sci U S A. 1999;96:4592–7.
21. Jaboin J, Wild J, Hamidi H, Khanna C, Kim CJ, Robey R, *et al*. MS-27-275, an inhibitor of histone deacetylase, has marked in vitro and in vivo antitumor activity against pediatric solid tumors. Cancer Res. 2002;62:6108–15.
22. Bridle BW, Chen L, Lemay CG, Diallo JS, Pol J, Nguyen A, *et al*. HDAC inhibition suppresses primary immune responses, enhances secondary immune responses, and abrogates autoimmunity during tumor immunotherapy. Mol Ther. 2013;21:887–94.
23. Shen L, Ciesielski M, Ramakrishnan S, Miles KM, Ellis L, Sotomayor P, *et al*. Class I histone deacetylase inhibitor entinostat suppresses regulatory T cells and enhances immunotherapies in renal and prostate cancer models. PLoS One. 2012;7:e30815.
24. Berghuis D, Schilham MW, Vos HI, Santos SJ, Kloess S, Buddingh EP, *et al*. Histone deacetylase inhibitors enhance expression of NKG2D ligands in Ewing sarcoma and sensitize for natural killer cell-mediated cytolysis. Clin Sarcoma Res. 2012;2:8.
25. Hughes DP, Thomas DG, Giordano TJ, Baker LH, McDonagh KT. Cell surface expression of epidermal growth factor receptor and Her-2 with nuclear expression of Her-4 in primary osteosarcoma. Cancer Res. 2004;64:2047–53.
26. Bollard CM, Rossig C, Calonge MJ, Huls MH, Wagner HJ, Massague J, *et al*. Adapting a transforming growth factor beta-related tumor protection strategy to enhance antitumor immunity. Blood. 2002;99:3179–87.
27. Warrenand HS, Rana PM. An economical adaptation of the RosetteSep procedure for NK cell enrichment from whole blood, and its use with liquid nitrogen stored peripheral blood mononuclear cells. J Immunol Methods. 2003;280:135–8.
28. Denman CJ, Senyukov VV, Somanchi SS, Phatarpekar PV, Kopp LM, Johnson JL, *et al*. Membrane-bound IL-21 promotes sustained

ex vivo proliferation of human natural killer cells. PLoS One. 2012;7: e30264.
29. Gore L, Rothenberg ML, O'Bryant CL, Schultz MK, Sandler AB, Coffin D, *et al*. A phase I and pharmacokinetic study of the oral histone deacetylase inhibitor, MS-275, in patients with refractory solid tumors and lymphomas. Clin Cancer Res. 2008;14:4517–25.
30. Man TK, Chintagumpala M, Visvanathan J, Shen J, Perlaky L, Hicks J, *et al*. Expression profiles of osteosarcoma that can predict response to chemotherapy. Cancer Res. 2005;65:8142–50.
31. Kato Y, Yoshimura K, Shin T, Verheul H, Hammers H, Sanni TB, *et al*. Synergistic in vivo antitumor effect of the histone deacetylase inhibitor MS-275 in combination with interleukin 2 in a murine model of renal cell carcinoma. Clin Cancer Res. 2007;13:4538–46.
32. Schmudde M, Braun A, Pende D, Sonnemann J, Klier U, Beck JF, *et al*. Histone deacetylase inhibitors sensitize tumour cells for cytotoxic effects of natural killer cells. Cancer Lett. 2008;272:110–21.
33. Khan N, Jeffers M, Kumar S, Hackett C, Boldog F, Khramtsov N, *et al*. Determination of the class and isoform selectivity of small-molecule histone deacetylase inhibitors. The Biochemical Journal. 2008;409:581–9.
34. Ryan QC, Headlee D, Acharya M, Sparreboom A, Trepel JB, Ye J, *et al*. Phase I and pharmacokinetic study of MS-275, a histone deacetylase inhibitor, in patients with advanced and refractory solid tumors or lymphoma. J Clin Oncol. 2005;23:3912–22.
35. Bagatell R, Gore L, Egorin MJ, Ho R, Heller G, Boucher N, *et al*. Phase I pharmacokinetic and pharmacodynamic study of 17-N-allylamino-17-demethoxygeldanamycin in pediatric patients with recurrent or refractory solid tumors: a pediatric oncology experimental therapeutics investigators consortium study. Clin Cancer Res. 2007;13:1783–8.
36. Epling-Burnette PK, Bai F, Painter JS, Rollison DE, Salih HR, Krusch M, *et al*. Reduced natural killer (NK) function associated with high-risk myelodysplastic syndrome (MDS) and reduced expression of activating NK receptors. Blood. 2007;109:4816–24.
37. Varker KA, Terrell CE, Welt M, Suleiman S, Thornton L, Andersen BL, *et al*. Impaired natural killer cell lysis in breast cancer patients with high levels of psychological stress is associated with altered expression of killer immunoglobin-like receptors. J Surg Res. 2007;139:36–44.
38. Sconocchia G, Lau M, Provenzano M, Rezvani K, Wongsena W, Fujiwara H, *et al*. The antileukemia effect of HLA-matched NK and NK-T cells in chronic myelogenous leukemia involves NKG2D-target-cell interactions. Blood. 2005;106:3666–72.
39. Rao-Bindal K, Zhou Z, Kleinerman ES. MS-275 sensitizes osteosarcoma cells to Fas ligand-induced cell death by increasing the localization of Fas in membrane lipid rafts. Cell Death Dis. 2012;3:e369.
40. Rao-Bindal K, Koshkina NV, Stewart J, Kleinerman ES. The histone deacetylase inhibitor, MS-275 (Entinostat), downregulates c-FLIP, sensitizes osteosarcoma cells to FasL, and induces the regression of osteosarcoma lung metastases. Curr Cancer Drug Targets 2013;13:411–22.